Nat. Hazards Earth Syst. Sci. Discuss., 3, 6117–6148, 2015
www.nat-hazards-earth-syst-sci-discuss.net/3/6117/2015/
doi:10.5194/nhessd-3-6117-2015

Natural Hazards and Earth System Sciences Discussions
Open Access

The unrest of S. Miguel volcano (El Salvador, CA): installation of the monitoring network and observed volcano-tectonic ground deformation

A. Bonforte[1], D. Hernandez[2], E. Gutiérrez[2], L. Handal[2], C. Polío[2], S. Rapisarda[1], and P. Scarlato[3]

[1]Istituto Nazionale di Geofisica e Vulcanologia, Sezione di Catania – Osservatorio Etneo, Piazza Roma, 2 95123 Catania, Italy
[2]Ministerio de Medio Ambiente y Recursos Naturales, Kilómetro 5 1/2 Carretera a Santa Tecla, Calle y Colonia Las Mercedes, San Salvador, El Salvador
[3]Istituto Nazionale di Geofisica e Vulcanologia, Sezione di Sismologia e Tettonofisica, Via di Vigna Murata, 605 00143 Roma, Italy

Received: 1 August 2015 – Accepted: 13 September 2015 – Published: 9 October 2015

Correspondence to: A. Bonforte (alessandro.bonforte@ingv.it)

Published by Copernicus Publications on behalf of the European Geosciences Union.

The unrest of S. Miguel volcano (El Salvador, CA)
A. Bonforte et al.

Abstract

On 29 December 2013, the Chaparrastique volcano in El Salvador, close to the town of S. Miguel, erupted suddenly with explosive force, forming a more than 9 km high column and projecting ballistic projectiles as far as 3 km away. Pyroclastic Density Currents flowed to the north-northwest side of the volcano, while tephras were dispersed northwest and north-northeast. This sudden eruption prompted the local Ministry of Environment to request cooperation with Italian scientists in order to improve the monitoring of the volcano during this unrest. A joint force made up of an Italian team from the Istituto Nazionale di Geofisica e Vulcanologia and a local team from the Ministerio de Medio Ambiente y Recursos Naturales was organized to enhance the volcanological, geophysical and geochemical monitoring system to study the evolution of the phenomenon during the crisis. The joint team quickly installed a multi-parametric mobile network comprising seismic, geodetic and geochemical sensors, designed to cover all the volcano flanks from the lowest to the highest possible altitudes, and a thermal camera. To simplify the logistics for a rapid installation and for security reasons, some sensors were co-located into multi-parametric stations. Here, we describe the prompt design and installation of the geodetic monitoring network, the processing and results. The installation of a new ground deformation network can be considered an important result by itself, while the detection of some crucial deforming areas is very significant information, useful for dealing with future threats and for further studies on this poorly monitored volcano.

1 Introduction

The S. Miguel volcano, also known as Chaparrastique, is a symmetrical stratovolcano, which reaches 2130 m a.s.l. Its summit crater measures 800 m in diameter and 340 m in depth. The Pacayal volcano (currently inactive) is located 6 km NW from the S. Miguel edifice (Fig. 1).

Geographically, it is located in the department of San Miguel, in the eastern part of El Salvador, at coordinates 13.43143° N and 88.271468° W. The entire edifice belongs to the municipalities of San Miguel, Quelepa, Moncagua, Chinameca, San Jorge, San Rafael Oriente and El Tránsito.

Geologically, it belongs to the quaternary period (probably with an age of about 50 000 years), and is mainly made up of basaltic and andesitic rocks. However, the stratigraphy of the volcano is intercalated with plinian acid deposits (dacitic and rhyodacitic) of the Pacayal volcano. Lava flows and mafic scoria emitted through lateral fissures (Escobar et al., 2004) are evident on the flanks of the volcano; the occurrence of such lateral eruptions increases the hazard for the numerous people living on the volcano slopes and requiring a more dense monitoring on all around its flanks.

Tectonically, the volcano is located in the eastern segment of the Central Graben of the country, and it is crossed by local faults with a predominant NW–SE direction (see Fig. 1). A huge fault is located to the north, 10 km away from the volcano, with a predominant E–W direction, and it defines the forearc segment that interacts directly with the Cocos Plate. This fault is locally called "El Salvador Fault Zone (ESFZ)". The forearc sliver shows a regional movement relative to the Caribbean plate towards the northwest, with an average speed of about 15 ± 2 mm per year. (Correa-Mora et al., 2009; Alvarado et al., 2011)

According to the Ministry of Environment and Natural Resources of El Salvador, around 5000 people living on the northwestern flank of the volcano are those most exposed to the volcanic hazard.

In the last 1500 years, the S. Miguel volcano has undergone at least 25 small eruptions, being the most active volcano in the Salvadorean volcanic chain. Since 1867, there have been at least 15 explosive eruptions through the central crater (MARN, 2014). The Volcanic Explosive Index (VEI) estimated for that period has been set between 1 and 2 (Schiek, 2008). The latest eruption occurred on 29 December 2013, when the volcano ejected a moderate volume of ashes and ballistics through the central crater, damaging several crops on the northern flank and prompting the people working there to take flight.

It is also important to note that the volcanic hazard of S. Miguel is not confined to an eruptive episode involving lava and pyroclastic flows, gas emissions, etc., but also the instability of the steep slopes create a suitable scenario to the generate landslides, debris flows or mudslides. The NW, NE, SE, S and SW flanks show vestiges of such historical events. At present, the drainage system of the NW sector towards Las Placitas, La Piedra, Lotificación Hercules and Caserío La Cruz are being affected by this phenomenon that increases the hazard and needs to be monitored especially during unrest periods.

The aim of this paper is to describe the international co-operation to improve the monitoring during the crisis, the design and installation of the multi-parametric network, the processing of GPS data and the observed ground deformation. This is the very first experience of such complete a monitoring of this volcano; in particular, the geodetic network installed is available for future studies and crisis management and the ground deformation analyses here reported provide a useful first insights into defining the deforming areas of the volcano and their possible significance, where attention could be concentrated for monitoring.

2 Background

Ground deformation at S. Miguel volcano was studied by Schiek (2008), by applying radar interferometry. Earthquake activity was also studied thanks to a network of six broadband stations around the volcano. The management of the seismic network was carried out by the Servicio Nacional de Estudios Territoriales (SNET) of the Ministry of Environment and Natural Resources of El Salvador (MARN). The equipment recorded continuously from March 2007 to January 2008. The SAR data were available for the period from February 2007 to January 2008. The study suggested that the main volcanic activity occurs along a fault crossing the crater in a north–south

NHESSD
3, 6117–6148, 2015

direction, known as the San Miguel Fracture Zone (SMFZ, see Fig. 1). Schiek (2008) measured a long-term succession of ground inflation and subsidence during that period, recording a maximum inflation of 6 ± 0.1 cm before mid-October 2007. After this period a maximum deflation of 4 ± 0.1 cm was verified until January 2008. The seismic data were used to model the subsurface geometry of SMFZ, determining that during the inflation period there was an excess of pressure of about 0.05 MPa; for the deflation, a value of about −0.05 MPa was estimated.

3 Continuous GPS Station at S. Miguel volcano

During 2007 and 2008, in the framework of a long-term research project by MARN and the University of Wisconsin, Madison on earthquakes and tectonics, continuous GPS stations were installed close to the volcanoes of Santa Ana, San Salvador and San Miguel. In the particular case of San Miguel, the GPS station was installed on 27 June 2007, in the Piedra Azul village on the southwestern flank of the volcano (Fig. 2). The deployed equipment comprised Trimble dual-frequency receivers and zephyr geodetic antennas, configured to acquire data every 30 s (Fig. 3).

4 The 29 December 2013 eruption

At 10:30 a.m. (LT = UTC−6) Sunday, 29 December 2013, the Chaparrastique volcano suddenly erupted, forming a column that reached an height of 9.7 km a.s.l. and ejecting ballistic projectiles as far as 3 km away (Fig. 4). Pyroclastic Density Currents (PDCs) flowed onto the north-northwestern side of the upper third of the volcanic edifice, and tephras were deposited toward the northwest and north-northeast areas. The pyroclastic currents and the fallout heavily damaged coffee plantations on the slopes of the volcano and frightened many people working there, forcing them to flee from the dense and suffocating ash cloud. The intense part of the eruptive phase lasted about 90 min. After the unrest, the volcano continued degassing, emitting around

1100 ton day^{-1} of SO_2 during the next fifteen days. Changes in amplitude of volcanic tremor were observed during the ten months following the eruption, and 15 small explosions were recorded until October 2014. These explosions reached a height of less than 1 km, and tiny ash fall deposits (mm in thickness) on the slopes of the volcano were observed. In Fig. 5, the tremor amplitude and the volcanic activity recorded during the period investigated by GPS measurements on the new network is reported.

5 New GPS network design and installation

On January 2014, a partnership of an Italian team (named V-EMER) from INGV (Istituto Nazionale di Geofisica e Vulcanologia) and a local team from MARN (Ministerio de Medio Ambiente y Recursos Naturales) was organized to improve the geochemical and geophysical multiparametric monitoring system after the 29 December 2014 eruption. The joint team installed on and around the volcano a mobile multi-parametric network that was shipped from Italy. It consisted of geochemical automatic stations, infrasound sensors, seismic broadband stations, radiometric sensors, GPS stations and also a thermal camera to monitor the northern side of the volcano and that, up to the time of writing, still provides real-time monitoring of the volcanic activity.

The installed ground deformation network was designed to cover the entire volcano from the lowest to the highest possible altitude. A detailed and optimal distribution of measuring points was required and designed to monitor not only the central part of the volcano but also its flanks due to the possibility of even more dangerous flank intrusions and/or slope stability. To simplify the logistics for the quickest installation and for security reasons, some GPS sensors, where possible, were co-located with already existing geophysical/geochemical stations (seismic, infrasound, gas plume and radiometric, example in Fig. 6).

The geodetic network consisted of 10 self-centering benchmarks of the same type usually installed on Mt. Etna in Italy (Puglisi and Bonforte, 2004; Bonforte and Puglisi, 2006); these benchmarks allow rapid installation and setup of the instrumentation

NHESSD
3, 6117–6148, 2015

and have a minimum impact. The benchmarks consist of brass cylinders that are permanently installed in solid outcrops (Fig. 7a) or stable reinforced concrete structures (Fig. 7b) by simply drilling a 5 cm wide hole and accurately fixing them with resin epoxy. Only for the highest VSMG benchmark, a cubic (50 cm sides) concrete block was buried in the pyroclastic material on the highest northern flank of the volcano (Fig. 8).

A screwed brass cap is usually closed and protects the benchmark when not in use. The internal part of the cylinders are designed to perfectly contain and fix, without any movement, the bottom of the geodetic pins that are screwed into them during the measurements. For this setup, 450 mm long aluminum pins were brought from Italy. The GPS antenna is then directly placed at the top of the vertical pin; the standard length and the fixed coupling between the benchmarks and the removable pins prevent any setup error (Fig. 9). This type of benchmark enables setting-up the station in less than a minute and even by personnel without any geodetic expertise. All geodetic benchmarks on and around Chaparrastique volcano were installed in two days, on 29 and 30 January. In order to start data acquisition as soon as possible, thanks to the very quick resin stabilization, helped by the high environmental temperatures, it was possible to setup all the GPS equipment on the new benchmarks on 30 January, just after the last benchmark installations.

The final configuration of the multi-parametric network installed by the joint international team is reported in Fig. 10. The GPS instrumentation comprised 10 Trimble dual-frequency receivers, model 4700, equipped with 4 Trimble Zephyr and 6 Leica AX1202GG antennas. All stations were powered with 40 Ah batteries and 20 W photovoltaic modules. Data were collected as daily files with a 30 s sampling interval.

Local personnel was also trained on how to manage, program, maintain and process the collected data to ensure the maximum efficiency and local autonomy in managing the ongoing crisis.

NHESSD
3, 6117–6148, 2015

6 Data acquisition and processing

Initially, a single 4 day survey was planned, to then be repeated during the following months in order to measure the station displacements. However, due to the continuous tremor increase during the measurements, we decided to keep all the GPS stations installed on the benchmarks in order to study the potential ground deformation accompanying the unrest episode. Due to the initial plans, data were stored locally in the memory of the sensors and were downloaded weekly by the MARN team. Stations were then removed at the end of April. Daily operation of the installed GPS stations and data availability is reported in Fig. 11.

Data from the Piedra Azul (VMIG) permanent GPS station were added to the processing to increase the number of stations on and around the volcano. This station lies on the volcano flank and cannot be chosen as a reference but it can be used for monitoring the volcano deformation. In order to refer the ground motion to a stable reference frame external to the volcano, we added the data from the far GUAT (Guatemala City), MANA (Managua), SSIA (San Salvador), ELEN (S. Elena), CN22 (Las Penitas) and CN23 (Belize) ITRF stations to the processing. Once final precise ephemeris were available weekly by IGS, each week of data were processed to achieve a unique coordinate for each station in the ITRF reference frame epoch 2014.1 (Altamimi et al., 2011). In this way, we obtained more robust point solutions and were able to overcome sporadic lack of data that sometimes affected some stations for short periods (a couple of days); only during the second week were SSIA station data lacking for the entire processed period (2–8 February, GPS week 1778, see Fig. 11).

The processing presented here was performed using the Trimble Business Center version 2.81, using the IGS final precise ephemeris and IGS absolute antenna calibration tables. Due to some anomalous interruptions in the data acquisitions, mainly owing to power failures, a first filter was applied and only baselines connecting stations with more than 8 h overlap were selected for processing. In this way, each processed network was made up of 17 stations and about 500 suitable baselines (Fig. 12). Each

NHESSD
3, 6117–6148, 2015

week of data, from GPS week 1778 to GPS week 1789, was processed as a whole and only fixed solutions were kept for the adjustment process; a first free (inner constrain) adjustment was performed in order to detect any noisy solution and then, after bad solutions were fixed or removed, a constrained adjustment was performed. Coordinates of the ITRF stations were fixed to their values in the ITRF08 frame at epoch 2014.1 (Altamimi et al., 2011). In this way, all station solutions on and around the volcano were referred to the same fixed frame and coordinate comparisons should reveal any local ground deformation within the ITRF reference and regional motion, following the approach of Bonforte and Guglielmino (2008).

Final 2σ positioning errors in the station coordinates were around 2–3 mm for the horizontal components and 4–5 mm for the vertical one.

7 Analysis of the ground deformation

Here, we show and analyze the weekly solutions of each station installed on the S. Miguel volcano. In Fig. 13, all the time series of the three components of motions are plotted for each station.

In general, there is no strong motion at the stations during the investigated period. An up-down behavior seems to characterize the first half of the period on most stations, followed by a more disturbed period, but the variations are often lower than the measurement errors.

Stations on the western flank appear to show a fluctuation in the horizontal components of motion just a few days after the tremor amplitude increase around the ash emission of 12 February 2014, roughly coinciding with the following steep decrease recorded from the end of January to the end of February. At LACA and VMIG stations, on the south-western side of the edifice, a slight general uplift could be recognized, more pronounced during the first half of the observed period.

In order to reduce the effects of common fluctuations of the positions due, for example, to reference system or atmospheric noise, the distance variations between station pairs were calculated and plotted, taking into account only the horizontal components in order to reduce the noise. In this way, the extension/contraction of different parts of the volcano can be analyzed with greater accuracy. The most interesting feature from this analysis is the detection of different areas of the volcano behaving differently in response to different dynamics.

The eastern side of the volcano, in fact, shows an interesting fairly continuous contraction clearly evidenced by the shortening of about 1 cm from BEMI to TANQ, from TANQ to MOPG and about 1.5 cm from PATI to TANQ (Fig. 14); the fairly constant rate of contraction suggests tectonic dynamics control this side of the volcano, especially on its eastern to south-eastern flank, due to the stability of the distances between BEMI, PATI and MOPG stations. A similar behavior appears on the opposite flank of the volcano, affecting the distances from PATI to RANC and VSMG, while the PATI-BEMI distance seems to show only a very slight and less constant contraction. In any case, on most of the time series a marked contraction is visible around the 12 February ash emission and, on all distance variations, another contraction marks the 12 April one. Longer time series in the future will evidence and eventually confirm this kind of almost linear deformation.

Distances between the stations located on the summit part (Fig. 15) seem to evidence a slight deflation/inflation behavior encompassing the tremor increase and ash emission of 12 February and 12 April. In particular, a deflation accompanied the tremor increase in February and a subsequent inflation affected the summit area after the ash emission until about the first half of March 2014; then a new slight inflation started, culminating roughly with the new 12 April ash emission. This deformation is very local, affecting the summit part of the volcano and is confirmed by the opposite behavior of the “radial” distances involving the same stations at lower altitudes not lying on opposite sides of the volcano. Distances from SJOR to LACA and from VSMG to BEMI, in fact, extend before the 12 February ash emission and contract immediately after. VSMG-BEMI distance also evidences another significant extension episode, roughly corresponding to a temporary increase of tremor amplitude recorded at mid-March (see Fig. 5) with a following contraction culminating with the 12 April ash emission. It is interesting to note the significant increase of the distances from VSMG and RANC to LACA following the 12 February ash emission, indicating a relative motion of LACA confirmed by the shortening of its distance to SJOR.

Looking at the baselines radially crossing the volcano (Fig. 16), it would be possible to infer the overall large-scale behavior of the edifice. It is interesting to note that the N–S distance, i.e. PATI-VMIG, is more sensitive to the volcanic dynamics with respect to the E–W SJOR-BEMI and SJOR-MOPG ones. Indeed, it shows the same deflation/inflation cycle around the 12 February ash emission and also another contraction episode at mid-March, with a specular behavior with respect to the VSMG-BEMI distance (see Fig. 15). Only E–W distances involving summit stations can be sensitive to the volcanic dynamics, as evidenced by the LACA-BEMI and RANC-BEMI ones, due to the same dynamics described in Fig. 15; they show an inflation during the mid-March tremor increase, with an opposite behavior with respect to the N–S PATI-VMIG distance, and a following long-term deflation leading to the 12 April ash emission.

Looking at the rest of the edifice (Fig. 17), the southern flank seems to be the most stable side of the volcano, showing no significant deformation during the monitored period, while the western flank evidences some fluctuations similar to those observed on the other long baselines of Fig. 16; in particular, the SJOR-VMIG distances shows a fluctuation accompanying the mid-march tremor increase similar to what observed, with higher amplitude on the RANC-BEMI and LACA-BEMI baselines crossing the edifice (Fig. 16). A significant variation following the 12 February ash emission, similar to what observed in Fig. 15, is also visible. Here, a contraction affects the south-western SJOR-VMIG baselines and an extensions affects the north-eastern SJOR-PATI and PATI-LACA ones, confirming the motion of LACA and suggesting an extension of this deformation, with a decreasing amplitude, on the south-western flank down to SJOR, evidencing with a better accuracy the horizontal motion visible in Fig. 13. Coupling the information coming from the baselines variations visible in Figs. 15 and 17 and the uplift plotted in Fig. 13, we can infer that a local inflation affected the upper WSW flank of the volcano after the 12 February ash emission.

8 Conclusions

This work focuses on the international co-operation, prompted by the Ministerio de Medio Ambiente y Recursos Naturales of El Salvador, with the Italian V-EMER team from the Istituto Nazionale di Geofisica e Vulcanologia, to implement a multi-parametric monitoring network for managing the crisis after the unrest of S. Miguel volcano. Particular emphasis is given here to the ground deformation network design, installation and data analyses.

The installation of a new ground deformation monitoring network by means of self-centering benchmarks can be considered a first permanent result, with 10 geodetic benchmarks installed on and around the volcano and available to deal with future threats and for studying and monitoring this poorly known but hazardous volcano.

In addition, data analyses presented here provide very important and new information on the ground deformation affecting S. Miguel volcano. Even if data inversion and modeling was not possible due to the slight deformation, we were able to detect and define different sectors of the edifice affected by diverse ground deformation patterns. We can summarize all the observations of ground deformation in the following points, defining some characteristic features that can be useful to appropriately plan and interpret future monitoring of the volcano:

1. A general and continuous contraction affects the N–S baselines on the south-eastern and northern sides of S. Miguel volcano, probably imputable to tectonic dynamics due to its fairly constant rate.

2. The stations at highest altitude are the most sensitive to the dynamics accompanying the eruptive activity, indicating that the magma dynamics mainly involves the upper part of the feeding system.

NHESSD
3, 6117–6148, 2015

3. Long E–W baselines are fairly stable, while long N–S ones show some fluctuations; these latter, as well as the short E–W ones involving summit stations, show long-term variations that seem related to the tremor amplitude fluctuations and volcanic activity.

On a positive note, a productive teamwork has begun with this international cooperation and local personnel has been trained in network installation and data management.

Author contributions. All the Authors participated to the fieldwork for installing the multi-parametric network and setting up the instrumentation; in particular, A. Bonforte was responsible for the ground deformation network and S. Rapisarda for the seismic one. P. Scarlato coordinated the team during the fieldwork. E. Gutierrez is expert on the geology and tectonics of the area. D. A. Hernandez managed the GPS network and with C. Polìo and L. Handal downloaded the data and maintained the instruments while installed in the field. A Bonforte performed the ground deformation analyses and coordinated the writing of the manuscript.

Acknowledgement. The authors wish to thank the Minister for the Environment of El Salvador H. Rosa and also C. Kattan, S. Gresta, E. Privitera, P. Papale for making this cooperation possible and for funding the Italian mission, the Italian embassy in El Salvador and the Italian Ambassador T. Barucco for her personal interest. We are also grateful to all the INGV V-EMER group, technical staff of MARN and, in particular, to D. Escobar, F. Montalvo, L. Mixco, R. Castro, N. Galvez, G. Giuffrida, A. La Spina, M. Liuzzo, G. Salerno for the difficult field operations. Thanks are due to S. Conway for reviewing the manuscript for language and grammar. Thanks are also due to all the Italian colleagues who prepared all the equipment in Italy to be shipped for this cooperation.

References

Altamimi, Z., Collilieux, X., and Métivier, L.: ITRF2008: an improved solution of the international terrestrial reference frame, J. Geodesy., 85, 457–473, doi:10.1007/s00190-011-0444-4, 2011.

NHESSD
3, 6117–6148, 2015

Alvarado, D., DeMets, C., Tikoff, B., Hernández, D., Wawrzyniec, T., Pullinger, C., Rodríguez, M., and Tenorio, C.: Forearc motion and deformation between El Salvador and Nicaragua: GPS, seismic, structural, and paleomagnetic observations, Lithosphere, 3, 3–21, doi:10.1130/L108.1, 2011.

Bonforte, A. and Guglielmino, F.: Transpressive strain on the Lipari-Vulcano volcanic complex and dynamics of the "La Fossa" cone (Aeolian Islands, Sicily) revealed by GPS surveys on a dense network, Tectonophysics, 457, 64–70, doi:10.1016/j.tecto.2008.05.016, 2008.

Bonforte, A. and Puglisi, G.: Dynamics of the eastern flank of Mt. Etna volcano (Italy) investigated by a dense GPS network, J. Volcanol. Geoth. Res., 153, 357–369, doi:10.1016/j.jvolgeores.2005.12.005, 2006.

Correa-Mora, F., DeMets, C., Alvarado, D., Turner, H. L., Mattioli, G., Hernandez, D., Pullinger, C., Rodriguez, M., and Tenorio, C.: GPS-derived coupling estimates for the Central America subduction zone and volcanic arc faults: El Salvador, Honduras and Nicaragua, Geophys. J. Int., 179, 1279–1291, doi:10.1111/j.1365-246X.2009.04371.x, 2009.

Escobar, D., Ferres, D., Pullinger, C., Delgado, H., Farraz, I., Alatorre, M., and Hurst, A.: Memoria Técnica de los Mapas de Escenarios de Amenaza Volcánica. Volcán de San Miguel o Chaparrastique, available at: http://www.snet.gob.sv/Geologia/Vulcanologia/memorias/mtVSM.htm, last access: 9 March 2012, 2004.

MARN: Cronología de Erupciones Volcán de San Miguel, Miguel, available at: http://www.snet.gob.sv/ver/vulcanologia/monitoreo/historial+eruptivo/fiid_volcan=7, 2014.

Puglisi, G. and Bonforte, A.: Dynamics of Mount Etna Volcano inferred from static and kinematic GPS measurements, J. Geophys. Res., 109, B11404, doi:10.1029/2003JB002878, 2004.

Schiek, C.: Characterizing the deformation of reservoirs using Radar, Interferometry, Gravity and Seismic Analysis, Ph.D. thesis, The University of Texas at El Paso, TX, USA, 2008.

NHESSD

3, 6117–6148, 2015

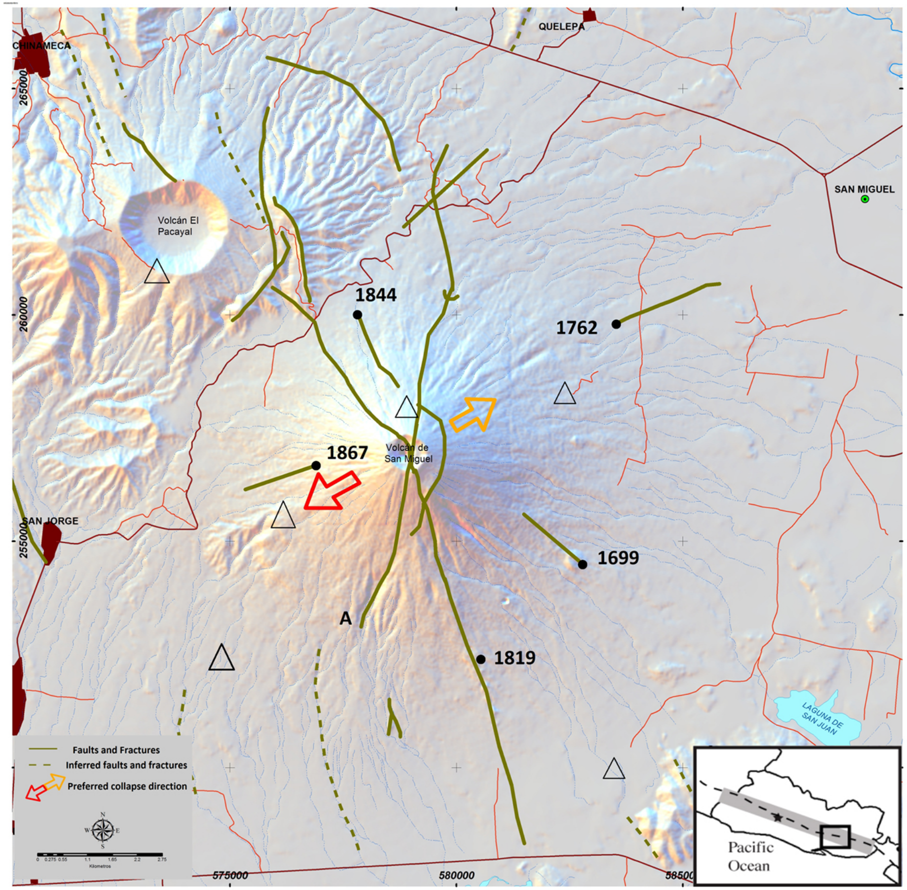

Figure 1. Tectonics and geodynamics of the S. Miguel volcano. The SMFZ is identified with A. The triangles show the installed seismometers. The circles mark the historical eruptions. Taken from Schiek (2008).

Figure 2. GPS hut located close to S. Miguel volcano.

NHESSD

3, 6117–6148, 2015

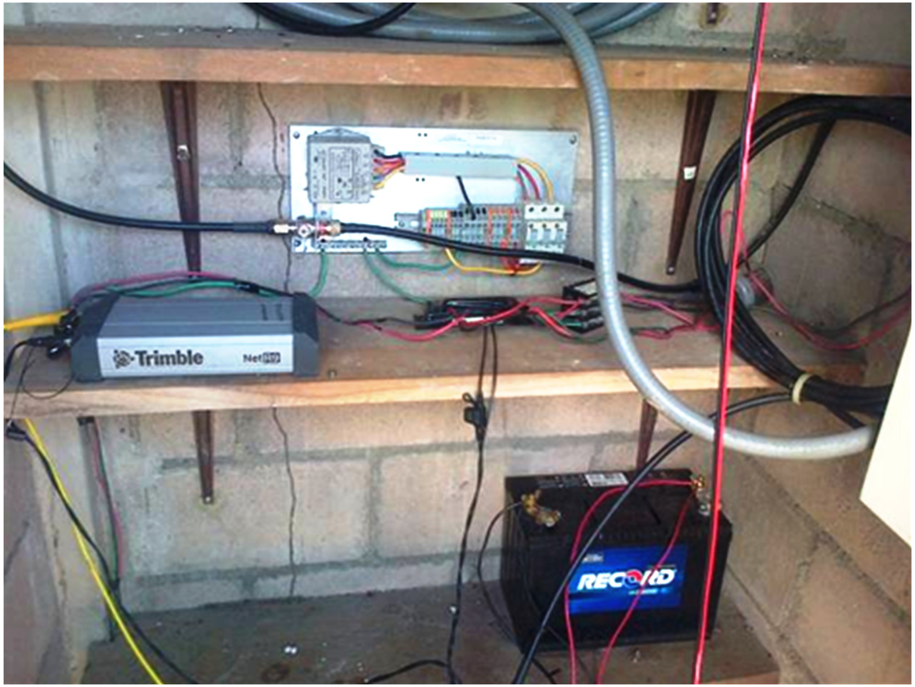

Figure 3. GPS receiver installed at S. Miguel volcano.

Figure 4. Shots of the 29 December 2013 eruption.

NHESSD
3, 6117–6148, 2015

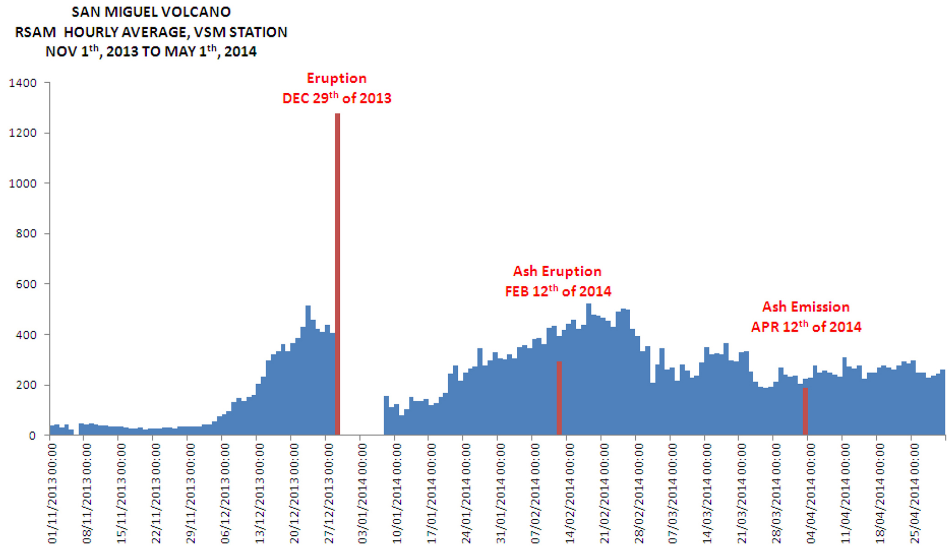

Figure 5. Eruption of 29 December 2013 and small explosions. The blue lines show the RSAM behavior during 2014 and the first days of 2015.

NHESSD
3, 6117–6148, 2015

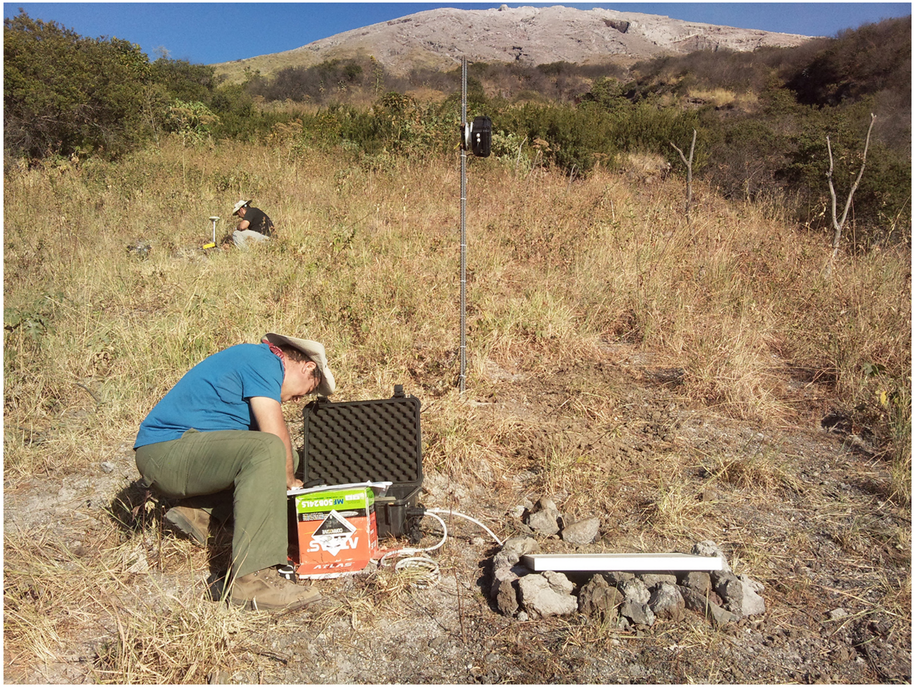

Figure 6. Ranchito multi-parametric station. Seismic station in the foreground; the radiometer is installed on the pole in the image center; the GPS station is visible a few meters further up.

NHESSD
3, 6117–6148, 2015

Figure 7. Installation of **(a)** Lacayo benchmark on rocky lava outcrop and **(b)** Tanque benchmark on existing reinforced concrete structure.

Figure 8. VSMG station, installed on the upper northern flank of the volcano, made by a reinforced concrete cube buried in the pyroclastic material, where the self-centering benchmark was anchored.

NHESSD
3, 6117–6148, 2015

Figure 9. Close-up of the self-centering mount at the Usulutan site and training of the MARN personnel in the field.

NHESSD
3, 6117–6148, 2015

NHESSD
3, 6117–6148, 2015

The unrest of S. Miguel volcano (El Salvador, CA)

A. Bonforte et al.

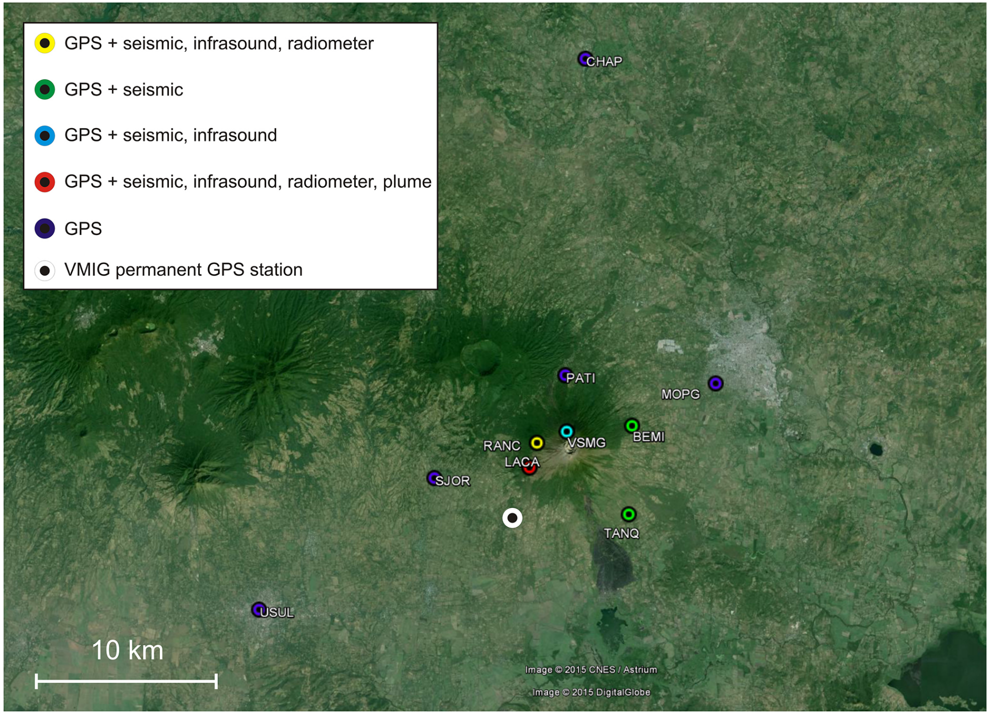

Figure 10. Map of the multi-parametric network installed in January 2014.

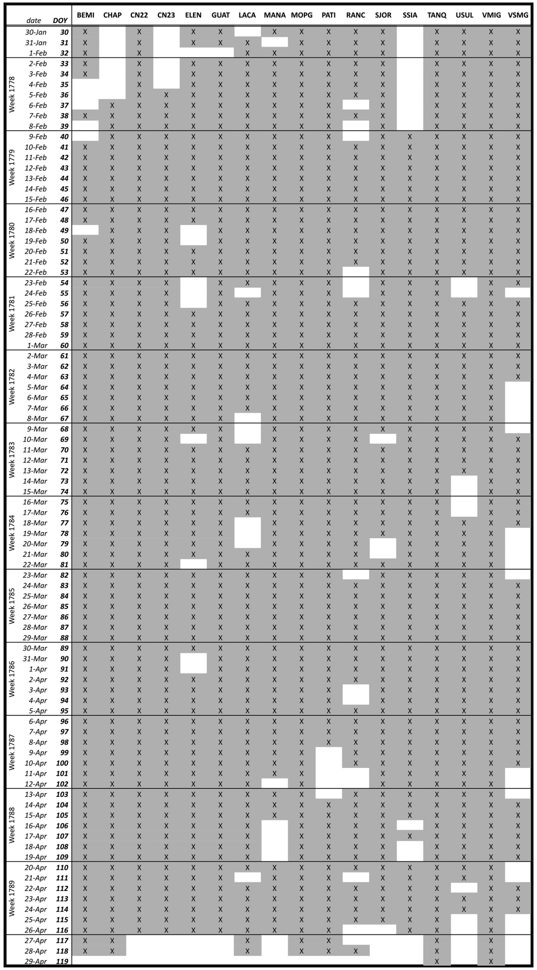

Figure 11. Continuity of data acquisition at the GPS stations used for the weekly processing.

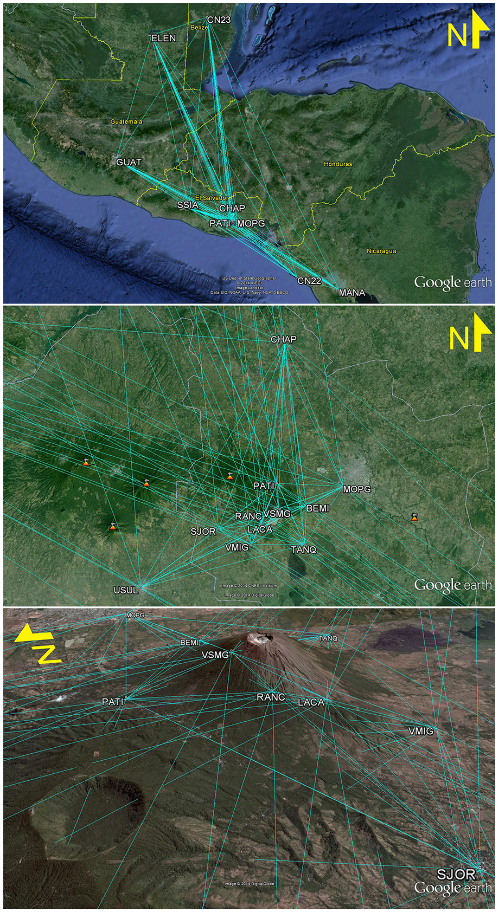

Figure 12. GPS network and baselines processed weekly for this work, from regional to local scale.

NHESSD

3, 6117–6148, 2015

The unrest of S. Miguel volcano (El Salvador, CA)

A. Bonforte et al.

Title Page
Abstract | Introduction
Conclusions | References
Tables | Figures
◂◂ | ▸▸
◂ | ▸
Back | Close
Full Screen / Esc
Printer-friendly Version
Interactive Discussion

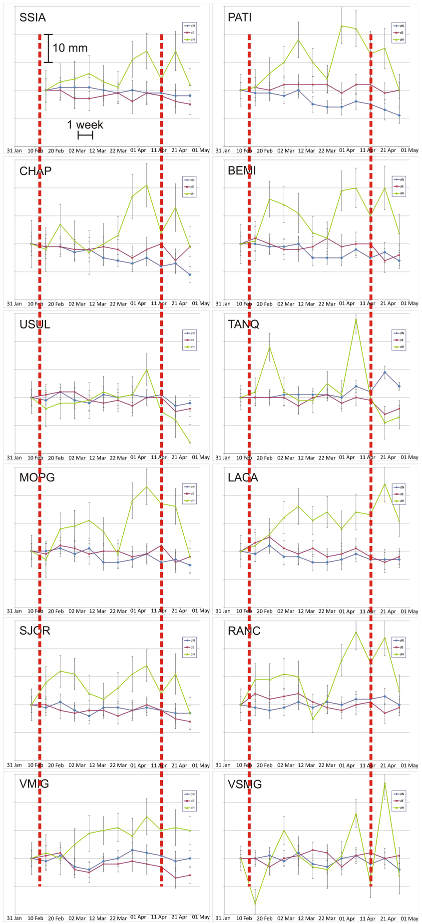

Figure 13. Weekly time series of the 3 components of displacements at the GPS stations. Vertical dashed lines indicate the occurrence of small ash emissions at S. Miguel volcano.

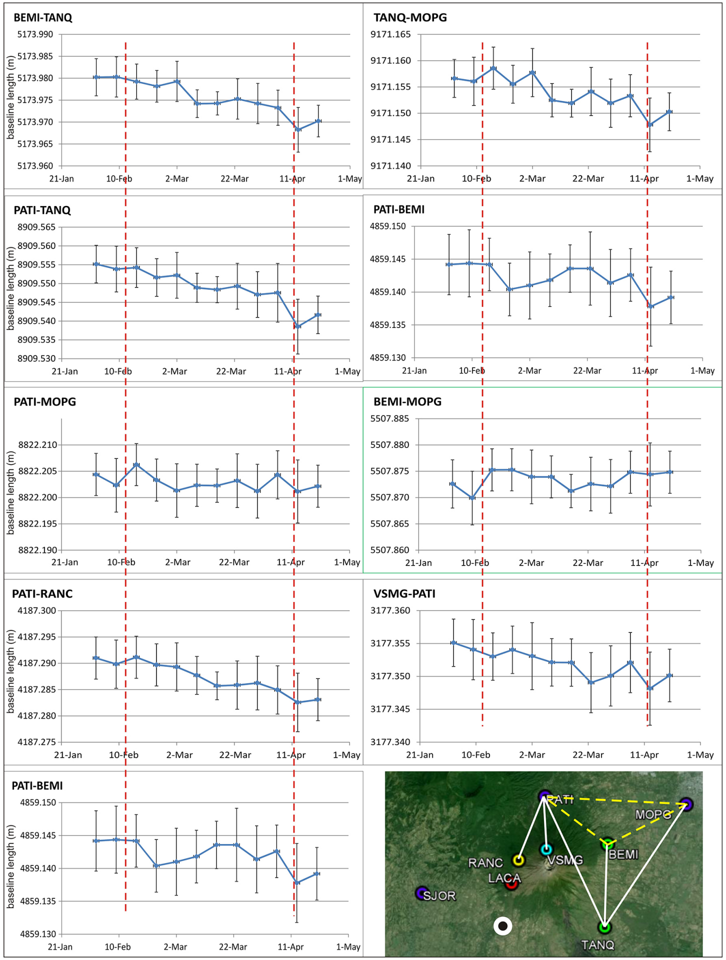

NHESSD
3, 6117–6148, 2015
The unrest of S. Miguel volcano (El Salvador, CA)
A. Bonforte et al.

Title Page
Abstract
Introduction
Conclusions
References
Tables
Figures
◀
▶
Back
Close
Full Screen / Esc
Printer-friendly Version
Interactive Discussion

Figure 14. Baseline length variations (meters) between stations lying on the eastern and northern sides of the volcano. The map shows the location and kinematics of the baselines: white solid lines indicate contracting distances; yellow dashed lines indicate the baselines showing no significant variations.

NHESSD
3, 6117–6148, 2015

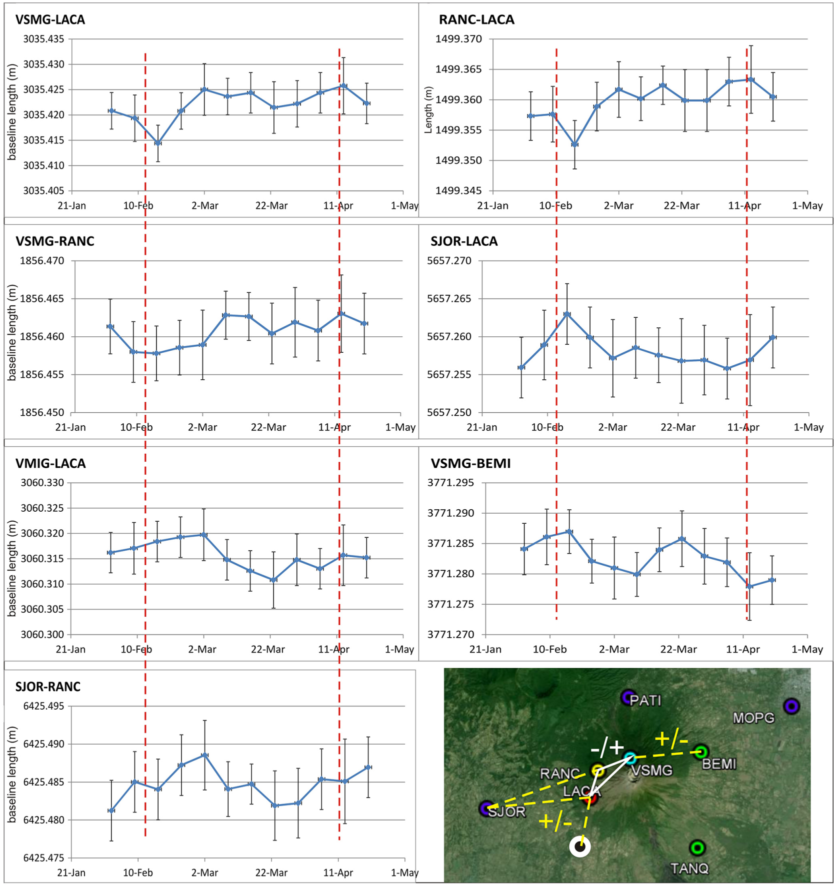

Figure 15. Baseline length variations (meters) evidencing the dynamics mainly affecting the summit part of the volcano. The map shows the location and kinematics of the baselines: when only the summit part extends (white solid lines), this produces contraction on the lower flanks (yellow dashed lines) and vice-versa.

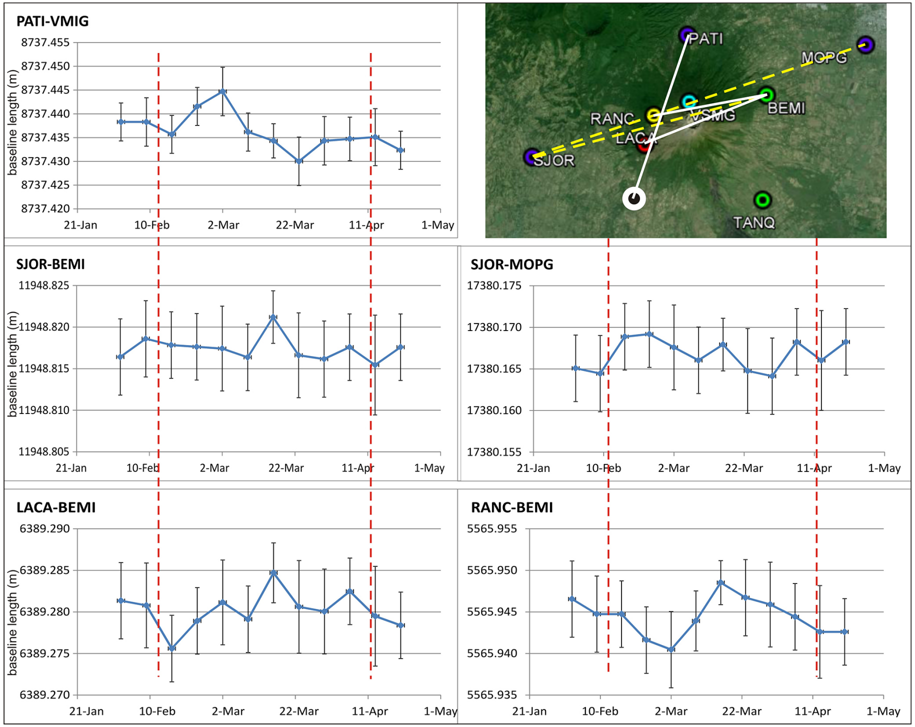

Figure 16. Variations of long length baselines (meters) crossing the volcano. The map shows the location and kinematics of the baselines: white solid lines indicate baselines showing significant fluctuations; yellow dashed lines indicate baselines showing no deformation.

NHESSD
3, 6117–6148, 2015

Title Page
Abstract | Introduction
Conclusions | References
Tables | Figures
◀| |▶
◀ ▶
Back | Close
Full Screen / Esc
Printer-friendly Version
Interactive Discussion

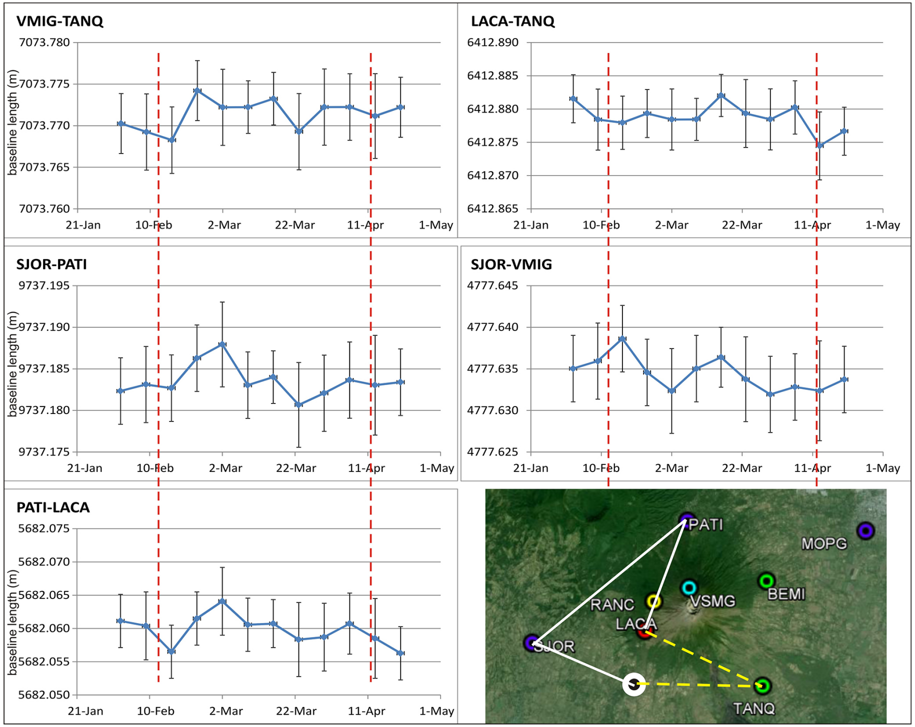

Figure 17. Baseline length variations (meters) between stations lying on the southern and western sides of the volcano. The map shows the location and kinematics of the baselines: white solid lines indicate fluctuating distances; yellow dashed lines indicate the baselines showing no significant variations.

NHESSD
3, 6117–6148, 2015